Published online April 19, 2004

2138–2146 *Nucleic Acids Research, 2004, Vol. 32, No. 7*
DOI: 10.1093/nar/gkh539

Mutual interactions between subunits of the human RNase MRP ribonucleoprotein complex

Tim J. M. Welting, Walther J. van Venrooij and Ger J. M. Pruijn*

Department of Biochemistry, Nijmegen Center for Molecular Life Sciences, University of Nijmegen, Nijmegen, The Netherlands

Received January 23, 2004; Revised and Accepted March 23, 2004

ABSTRACT

The eukaryotic ribonuclease for mitochondrial RNA processing (RNase MRP) is mainly located in the nucleoli and belongs to the small nucleolar ribonucleoprotein (snoRNP) particles. RNase MRP is involved in the processing of pre-rRNA and the generation of RNA primers for mitochondrial DNA replication. A closely related snoRNP, which shares protein subunits with RNase MRP and contains a structurally related RNA subunit, is the pre-tRNA processing factor RNase P. Up to now, 10 protein subunits of these complexes have been described, designated hPop1, hPop4, hPop5, Rpp14, Rpp20, Rpp21, Rpp25, Rpp30, Rpp38 and Rpp40. To get more insight into the assembly of the human RNase MRP complex we studied protein–protein and protein–RNA interactions by means of GST pull-down experiments. A total of 19 direct protein–protein and six direct protein–RNA interactions were observed. The analysis of mutant RNase MRP RNAs showed that distinct regions are involved in the direct interaction with protein subunits. The results provide insight into the way the protein and RNA subunits assemble into a ribonucleoprotein particle. Based upon these data a new model for the architecture of the human RNase MRP complex was generated.

INTRODUCTION

RNase MRP was originally identified as an endoribonuclease able to cleave an RNA substrate derived from the mitochondrial origin of DNA replication *in vitro* (1). Consequently, a role for RNase MRP in the priming of mitochondrial DNA replication was proposed. Later, it was found that the majority of the cellular RNase MRP pool was localized in the nucleolus (2,3), where it was shown to cleave the precursor rRNA *in vitro*, thereby contributing to the maturation of the 5′ end of 5.8S rRNA (4). The characterization of the murine RNase MRP particle showed that it contains an RNA species (also referred to as Th or 7-2 RNA) that is required for its enzymatic activity (5). RNase MRP RNA is nuclear encoded and classified as a small nucleolar RNA (snoRNA). SnoRNAs exist in the nucleolus as small nucleolar ribonucleoprotein complexes (snoRNPs). These complexes are involved in various steps of ribosomal RNA biosynthesis (6,7). Based on structural and functional differences, three classes of snoRNPs can be discerned. Box C/D snoRNPs are involved in 2′-*O*-methylation and endonucleolytic cleavage (8); box H/ACA snoRNPs mediate pseudouridinylation (9) and RNase MRP and the related RNase P are involved in endonucleolytic processing events (10). RNase MRP shares both functional and structural features with RNase P (10,11). RNase P is involved in the processing of pre-tRNA. Like the RNase MRP particle, the RNase P particle contains an essential RNA subunit, also referred to as H1 or 8-2 RNA. Although the sequences of both RNA subunits are not highly conserved, they can be folded into similar secondary structures (12,13). Furthermore, both complexes share protein subunits that co-purify with the respective endoribonuclease activities. RNase P is ubiquitously present in every investigated organism, whereas RNase MRP is restricted to eukaryotes. The conserved properties of both complexes strongly suggest that they have evolved from a common prokaryotic ancestor (14). RNase MRP was previously shown to be involved in the ancient recessive pleiotropic human disease cartilage hair hypoplasia (CHH) (15,16). In patients with CHH, the gene encoding the RNA subunit of RNase MRP (RMRP) is mutated. In the coding region of a predominant CHH-associated allele, the adenine on position 70 is substituted by guanine. This 70 A→G mutation was shown to be the cause of CHH. In other patients the RMRP gene displays other nucleotide substitutions and small sequence duplications. The effect of these mutations on the function of the human RNase MRP complex is not known yet.

Many studies have addressed the protein composition of the RNase MRP and RNase P complexes. Proteins that co-purify with human RNase MRP and RNase P are: hPop1, hPop4 (also designated Rpp29), hPop5, Rpp14, Rpp20, Rpp21, Rpp25, Rpp30, Rpp38 and Rpp40 (17–24). Some insight into the intermolecular interactions between the human RNase MRP RNA and a limited number of protein subunits (Rpp20, Rpp25, Rpp38 and hPop1) was previously provided (25). Recently, additional data on mutual subunit–subunit interactions generated by yeast two- and three-hybrid analyses for components of both the human and *Saccharomyces cerevisiae* RNase P became available (26–28). In this study, we have

*To whom correspondence should be addressed at Department of Biochemistry 161, University of Nijmegen, PO Box 9101, NL-6500 HB Nijmegen, The Netherlands. Tel: +31 24 361 6847; Fax: +31 24 354 0525; Email: g.pruijn@ncmls.kun.nl

systematically investigated direct intermolecular interactions between the human RNase MRP subunits using a GST pull-down assay. These experiments identified 19 strong and six weak protein–protein interactions. In addition, six out of eight GST-fusion proteins exhibited RNase MRP RNA binding properties. The analysis of RNase MRP RNA deletion mutants provided more detailed information on the regions of the MRP RNA that are involved in the interactions with these proteins. The data obtained in this study, in combination with previously published data, were used to generate a structural model for the human RNase MRP complex.

MATERIALS AND METHODS

GST-fusion proteins

To generate N-terminally GST-tagged fusion proteins, cDNAs encoding hPop1, hPop4, hPop5, Rpp14, Rpp20, Rpp21, Rpp25, Rpp30, Rpp38 and Rpp40 were cloned into pGEX-2T'G [derived from pGEX-2T (Amersham Pharmacia Biotech), containing a modified multiple cloning site]. The construct encoding GST-hRrp42p was kindly provided by David Tollervey (University of Edinburgh, UK). GST-fusion proteins were produced in *Escherichia coli* BL21(DE3)pLysS by standard procedures (29). Cell lysates were prepared by sonication of the bacteria in PBS using a Branson microtip. Subsequently, Triton X-100 was added to a final concentration of 1%. After centrifugation, the supernatants were used to isolate GST-fusion proteins by glutathione–Sepharose affinity chromatography. Glycerol was added to the GST-fusion protein containing fractions to a final concentration of 10%. The purity and quantity of the recombinant proteins were determined by SDS–PAGE.

In vitro translation of RNase MRP proteins

hPop1, hPop4, hPop5, Rpp14, Rpp20, Rpp21, Rpp25, Rpp30, Rpp38 and Rpp40 cDNAs were cloned into the pCI-neo vector (Promega) in-frame with a sequence encoding the vesicular stomatitis virus G protein epitope (VSV). Prior to *in vitro* translation, the constructs were linearized and mRNAs encoding the N-terminally VSV-tagged proteins were generated by *in vitro* transcription using T7 RNA polymerase. *In vitro* translation of the mRNAs was performed in a rabbit reticulocyte lysate translation system (Promega) in the presence of ^{35}S-methionine.

RNase MRP RNA constructs and *in vitro* transcription

RNase MRP constructs (MRP1–267, MRP1–82, MRP67–267, MRP67–197, MRP67–167, MRPΔ87–115) and a human Y1 RNA construct have been described previously and were linearized as described before (25,30). MRPΔ132–176 was generated by substituting the corresponding fragment of the wild-type construct (MRP1–267) with a PCR fragment lacking nucleotide 132–176. MRPΔ132–176 was linearized as described for MRP1–267. For *in vitro* transcription, 1 μg of linearized template DNA was incubated for 1 h at 37°C in 20 μl of buffer containing 40 mM Tris–HCl, pH 7.9, 6 mM $MgCl_2$, 2 mM spermidine, 10 mM NaCl, 10 mM dithiotreitol, 0.1 μg/μl bovine serum albumin, 40 U RNasin, 1 mM ATP, 1 mM GTP, 1 mM CTP, 0.1 mM UTP, 6.6 fmol (20 μCi) [α-^{32}P]UTP and 15 U T7 RNA polymerase. After transcription, RNA was purified by phenol/chloroform/isoamylalcohol extraction and by chromatography on a Sephadex G50 spin column.

GST pull-down assay

Ten microlitres of glutathione–Sepharose beads were washed three times with 100 μl of pull-down buffer [PB-100: 20 mM HEPES/KOH, pH 7.6, 100 mM KCl, 0.5 mM EDTA, 0.05% NP-40, 1 mM dithiotreitol, 5 mM $MgCl_2$, 0.02% BSA, Complete protease inhibitor (Roche)]. GST(-fusion) protein (5 pmol for protein–protein and 0.5 pmol for protein–RNA interactions) was coupled to the beads in 100 μl of PB-100 by incubating at room temperature for 30 min. After centrifugation, the supernatant was discarded and the beads were resuspended in pull-down buffer. For the analysis of protein–protein interactions, the beads were resuspended in 100 μl of PB-100. *In vitro* translated, ^{35}S-labelled protein was added and the mixture was incubated at 4°C for 2 h under continuous agitation. After incubation, the beads were washed three times with PB-150 (composition like PB-100, but containing 150 mM KCl) and the bound proteins were analysed by SDS–PAGE and autoradiography. For protein–RNA interaction analysis, the beads were resuspended in 100 μl of PB-200 (composition like PB-100, but containing 200 mM KCl and lacking $MgCl_2$). After the addition of *in vitro* transcribed ^{32}P-labelled RNAs, 2 μg of *Escherichia coli* tRNA and 20 U RNasin, the mixture was incubated for 1 h at 4°C under continuous agitation. The beads were washed three times with PB-200 and the co-precipitating RNAs were extracted and analysed by denaturing PAGE and autoradiography.

RESULTS

To shed more light on the architecture of the human RNase MRP complex, we investigated the mutual interactions between all currently known subunits. Protein–protein and protein–RNA interactions were investigated *in vitro* by a GST pull-down assay. The ORFs of all human RNase MRP proteins were cloned into the pGEX-2T'G expression vector. Subsequently, the GST–hPop1, GST–hPop4, GST–hPop5, GST–Rpp14, GST–Rpp20, GST–Rpp21, GST–Rpp25, GST–Rpp38 fusion proteins and, as controls, GST and GST–hRrp42p [a fusion protein of GST and the human exosome subunit hRrp42p (31)] were expressed in *E.coli* and purified by means of glutathione–Sepharose affinity chromatography (Fig. 1). Note that in addition to the full-length fusion proteins, the purified fractions, in particular those of GST–hPop1, GST–hPop4, GST–Rpp21 and GST–Rpp38, contained variable levels of faster migrating polypeptides, which presumably represent degradation products of the recombinant proteins. Several attempts to express the GST–Rpp30 and GST–Rpp40 fusion proteins were not successful.

Protein–protein interactions

The human RNase MRP protein subunits were produced by *in vitro* transcription/translation using a rabbit reticulocyte lysate system and ^{35}S-labelled methionine. SDS–PAGE analysis demonstrated that all of these were efficiently produced in the *in vitro* translation system (data not shown).

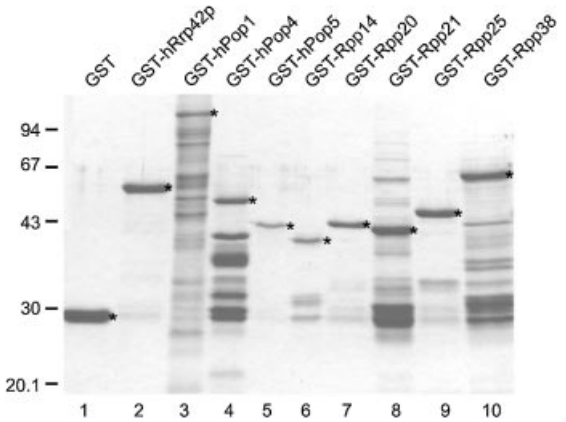

Figure 1. Recombinant GST-fusion proteins of RNase MRP subunits. The composition of the recombinant GST-fusion protein preparations was analysed by SDS–PAGE. The asterisks (*) indicate the full-length GST-(fusion) proteins. Lane 1, GST; lane 2, GST–hRrp42p; lane 3, GST–hPop1; lane 4, GST–hPop4; lane 5, GST–hPop5; lane 6, GST–Rpp14; lane 7, GST–Rpp20; lane 8, GST–Rpp21; lane 9, GST–Rpp25; lane 10, GST–Rpp38. The faster migrating polypeptides most likely represent truncated versions of the full-length recombinant proteins. The positions of molecular mass markers are indicated on the left.

The purified GST-fusion proteins were immobilized by binding to glutathione–Sepharose beads and incubated with each of the radiolabelled *in vitro* translated proteins. Radiolabelled proteins interacting with the GST-fusion proteins were analysed by SDS–PAGE and autoradiography. As controls for the specificity of these assays GST alone and GST–hRrp42p were used.

Using this approach a total of 18 efficient and seven less efficient protein–protein interactions were observed. The results of a few representative experiments are shown in Figure 2: efficient interactions (at least 20% of input protein co-precipitated) in Figure 2A–D and an example of a weak interaction (<20% of input) in Figure 2E. A complete set of experimental data is provided in a supplementary figure, which is published online. A summary of all interactions detected is shown in Figure 3. Six interactions were detected in 'two directions', i.e. with either one or the other interacting protein fused to GST. These interactions are hPop1–hPop4 (Fig. 2A and B), hPop4–hPop5, hPop4–Rpp38, hPop5–Rpp14, hPop4–Rpp25 and Rpp20–Rpp25. All the other interactions were only detected in one direction, which may be at least in part due to the fact that GST-fusion proteins of Rpp30 and Rpp40 were not available. In addition, this phenomenon may be explained by interference of the GST part of the recombinant protein with the interaction of the *in vitro* translated protein. Interestingly, hPop1, hPop4 and Rpp14 each displayed interactions with five other RNase MRP proteins (Fig. 3).

The interaction between Rpp20 and Rpp25 appeared to be the most efficient one observed in this assay (Fig. 2D). The strength of this interaction was substantiated by the fact that it was not affected by salt concentrations up to 3 M KCl (data not shown). The Rpp21 protein appeared to be a rather sticky protein, because in the GST pull-down assay both GST–Rpp21 and *in vitro* translated Rpp21 gave rise to relatively

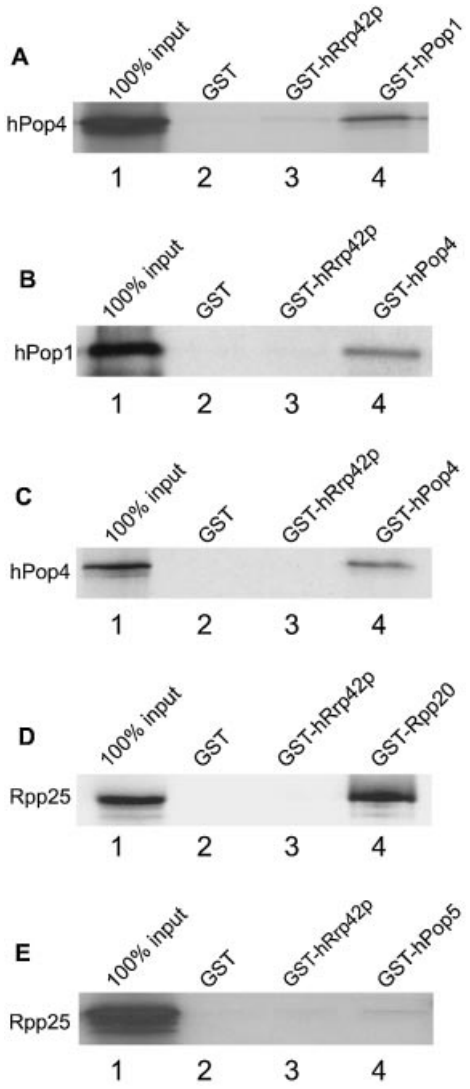

Figure 2. GST pull-down analysis of RNase MRP protein–protein interactions. GST-fusion proteins were incubated with ^{35}S-labelled *in vitro* translated proteins and after precipitation by glutathione–Sepharose, co-precipitated radiolabelled proteins were analysed by SDS–PAGE and autoradiography. In each panel, lane 1 shows the radiolabelled input protein, lanes 2 and 3 the negative control precipitations with GST and GST–hRrp42p, respectively, and lane 4 the material precipitated by the GST-tagged RNase MRP protein. (**A**) Interaction between GST–hPop1 and hPop4. (**B**) Interaction between GST–hPop4 and hPop1. (**C**) Interaction between GST–hPop4 and hPop4. (**D**) Interaction between GST–Rpp20 and Rpp25. (**E**) Interaction between GST–hPop5 and Rpp25.

high signals with all proteins, including the negative controls (GST and GST–hRrp42p). Raising the KCl concentrations to 150 mM resulted in the disappearance of these non-specific co-precipitations. Interestingly, under these conditions, the Rpp40 protein still interacted with GST–Rpp21. Several GST-tagged RNase MRP proteins, particularly hPop1 and hPop4 were observed to homodimerize with the corresponding *in vitro* translated protein in the GST pull-down assay. In Figure 2C, the result for the GST–hPop4–hPop4 interaction is shown. Besides homodimerization, the formation of multimers may also explain these results.

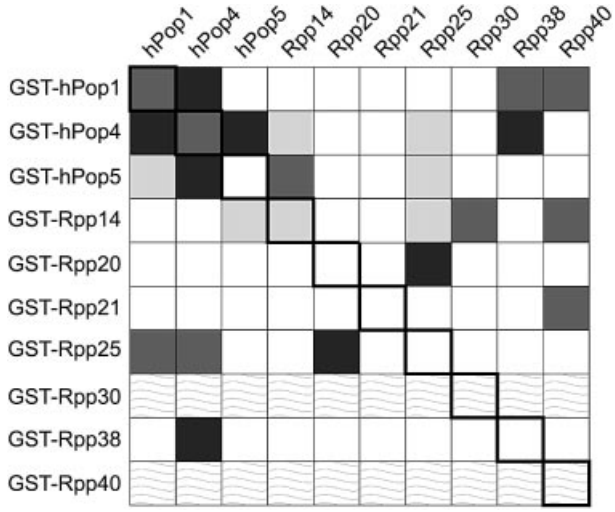

Figure 3. Summary of protein–protein interactions between the RNase MRP protein subunits detected by GST pull-down analyses. The dark-grey boxes indicate efficient interactions (more than 20% of input radiolabelled protein precipitated) that were detected with either one or the other interacting partner fused to GST; the grey boxes mark efficient interactions that were detected in only one of the reciprocal pull-downs; the light-grey boxes indicate relatively weak interactions (<20% of input protein precipitated). Because GST–Rpp30 and GST–Rpp40 were not available, these proteins were not analysed.

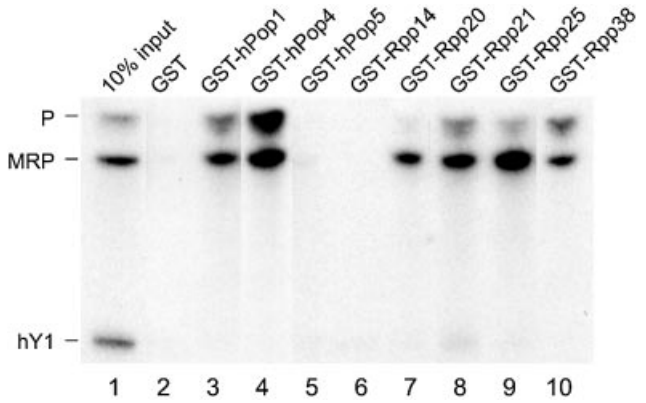

Figure 4. Direct interactions between GST-tagged RNase MRP proteins and the human RNase MRP and RNase P RNAs. The eight bacterially expressed GST-fusion proteins were incubated with a mixture of ^{32}P-labelled, *in vitro* transcribed, full-length human RNase MRP RNA, RNase P RNA and hY1 RNA, a small RNA associated with human Ro RNPs which was included as a negative control. Binding of these RNAs was determined by GST pull-down followed by denaturing gel electrophoresis of the co-precipitated RNAs and autoradiography. Ten percent of the input RNA was loaded in lane 1. The GST fusion proteins are indicated above the lanes (lanes 3–10). GST alone was used as a control (lane 2). The positions of RNase P RNA (P), RNase MRP RNA (MRP) and hY1 RNA (hY1) are indicated on the left.

Protein–RNA interactions

Because the RNA component of RNase MRP is expected to play a major role in assembly of the ribonucleoprotein particle, we next investigated direct interactions of protein subunits with the RNA. For these analyses GST pull-down experiments were performed with ^{32}P-labelled, *in vitro* transcribed RNA. First, the binding to full-length RNase MRP and RNase P RNA was examined. As shown in Figure 4, six of the GST-tagged RNase MRP protein subunits bound to both RNase MRP and RNase P RNA, whereas the remaining two proteins, GST–hPop5 and GST–Rpp14, did not show detectable binding. A control RNA, hY1 RNA, a small RNA associated with the cytoplasmic Ro RNPs, was not detectably precipitated by any of the GST-fusion proteins, except for GST–Rpp21, which resulted in weak hY1 RNA signals. The latter observation is most likely due to the sticky nature of Rpp21 (see above).

To investigate the regions of the RNase MRP RNA involved in the interactions with these proteins in more detail, mixtures of RNase MRP RNA deletion mutants (Fig. 5) were analysed for their protein-binding properties in the GST pull-down assay. To exclude the possibility that the use of RNA mixtures would affect the interaction behaviour of the deletion mutants, their protein-binding properties were also analysed in the GST pull-down assay separately. The results of these analyses were indistinguishable from those obtained with RNA mixtures. In Figure 6, a representative subset of the experimental data is shown. A complete set of experimental data is provided in a supplementary figure, which is published online. The results of these analyses are summarized in Figure 7. In agreement with their lack of interaction with the full-length RNase MRP RNA, GST-fusion proteins of hPop5 and Rpp14 did not show any interaction with either of the RNase MRP mutants. All truncations of the RNase MRP RNA except for MRPΔ87–115 reduced the efficiency of binding by hPop1. Deletions of nucleotides 1–66 and 132–176 only had a relatively small effect on hPop1 binding, whereas an additional deletion of nucleotides 198–267 more drastically affected the binding of this protein. Taken together, these data suggest that hPop1 contacts the RNase MRP RNA at multiple sites and that the P4 region may be critically important for its interaction. Rpp20 displayed a strong interaction with the mutant lacking nucleotides 132–176, but only weakly interacted with all the other mutants analysed, except for the P3 domain, which was bound only slightly less efficiently than the full-length RNA. These data suggest that for Rpp20 binding the P3 region and the P8/P9 region are important. Rpp25 showed efficient binding not only to the full-length RNA, but also to several mutants. Only a deletion of nucleotides 1–66 in combination with a deletion of nucleotides 198–267 significantly reduced Rpp25 binding. These data are consistent with the presence of two high-affinity binding sites for Rpp25 in the RNase MRP RNA, one situated in the P3 domain and another in the P4/P19 region. In addition to the full-length RNA, hPop4 also efficiently interacted with mutant RNAs lacking nucleotides 87–115 and 132–176. However, deletion of the nucleotides comprising the P3 domain reduced the binding efficiency of hPop4 drastically. The additional deletion of nucleotides 198–267 completely abrogated the interaction between hPop4 and the RNA. In agreement with the reduced binding of hPop4 with the mutant RNA lacking the P3 domain (MRP67–267), hPop4 showed an efficient interaction with MRP1–82. These data strongly suggest that hPop4 interacts with the MRP RNA by binding to more than one region of the RNA. As observed for Rpp25, both the P3 and the P4/P19 regions are important for hPop4 binding.

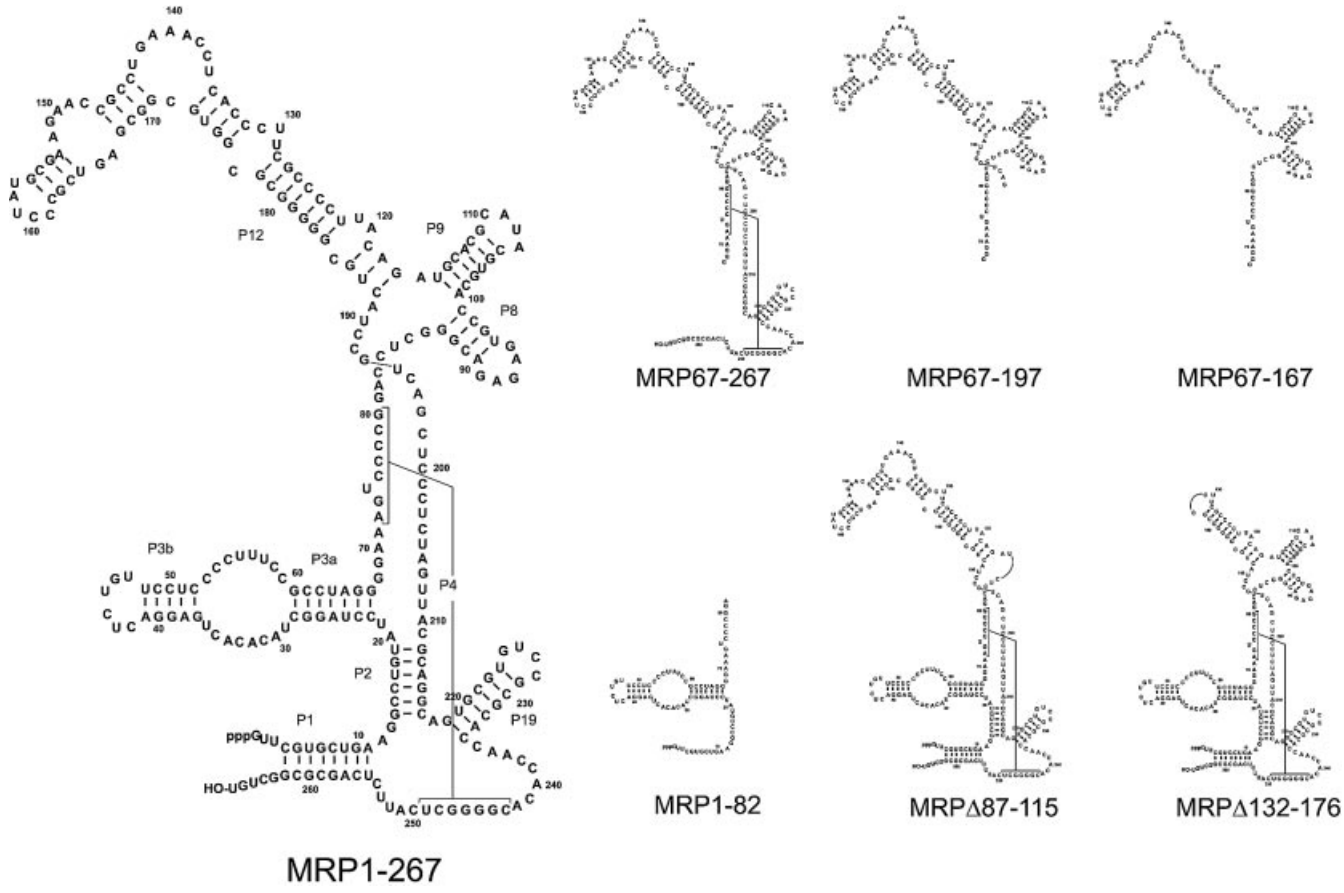

Figure 5. Schematic structure of deletion mutants of RNase MRP RNA. The RNA on the left represents the predicted secondary structure of the human RNase MRP RNA. The designations of the phylogenetically conserved helices (P1–P19) is based upon the RNase P RNA numbering described by Frank *et al.* (37). In the structures of the deletion mutants MRP67–267, MRP67–197, MRP67–167, MRP1–82, MRPΔ87–115 and MRPΔ132–176 only the remaining regions are shown.

Rpp38 efficiently interacted with the mutants lacking nucleotides 1–66 or 87–115 and somewhat less efficiently with mutants MRPΔ132–176 and MRP67–197. No or hardly any binding was observed for Rpp38 when the 3′ truncation was increased up to nucleotide 167 or to the isolated P3 domain. This indicates that Rpp38 binding is dependent on elements in the P12 domain, although the deletion of nucleotides 132–176 only partially decreased its binding efficiency. The interpretation of the data for Rpp21 is difficult, because this protein is known to display a sticky behaviour in interaction studies. Indeed, moderate binding to all RNase MRP mutants was observed. Therefore, no conclusions can be drawn for the binding of this protein to RNase MRP RNA.

DISCUSSION

Reconstitution of the RNase MRP complex will be required to unravel the role of the individual subunits in the endonucleolytic cleavage of substrate RNAs. As a first step towards *in vitro* reconstitution of this ribonucleoprotein particle, we have determined mutual interactions between its protein and RNA subunits. Using GST pull-down assays, we have detected 25 protein–protein and six protein–RNA interactions. At least one interaction with another subunit was found for each of the known subunits. These data can be used to build a model for the human RNase MRP complex (see below), which will provide a basis for its reconstitution using individual (recombinant) subunits.

Protein–protein interactions

A total of 19 distinct protein–protein interactions were detected, six of which were found when either one or the other interacting partner was fused to GST. Four of these (the interactions between hPop1 and hPop4, hPop4 and hPop5, hPop4 and Rpp38, and between Rpp20 and Rpp25), were not only detected when the two members of a particular pair of proteins were tested alternatively as GST-fusion protein, but also resulted in high GST pull-down efficiencies. Five interactions were supported only by weak signals and were not reciprocal. Using a yeast-two-hybrid assay, Jiang and Altman have studied interactions between all human RNase P/RNase MRP protein subunits, except for hPop5 and Rpp25 (26). Although they did not observe strong interactions, a series of weak interactions between pairs of these proteins were detected. A number of our GST pull-down data confirm these two-hybrid results. Taking into account that hPop5 and Rpp25 were not included in the yeast two-hybrid study, all but two of the interactions detected by GST pull-down were also

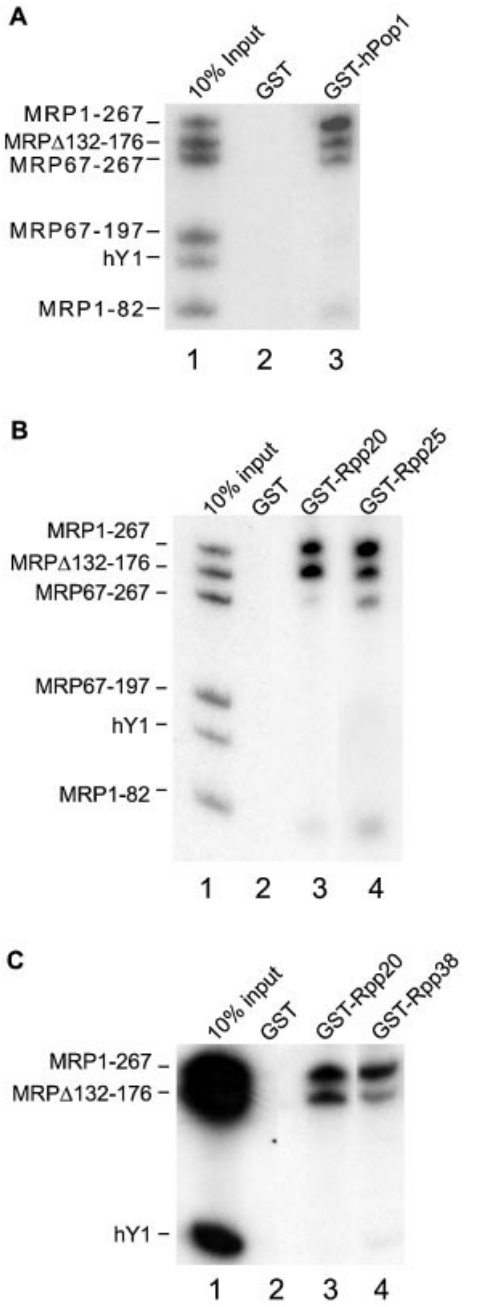

Figure 6. GST pull-down analysis of RNase MRP protein–RNA interactions. GST-fusion proteins were incubated with radiolabelled *in vitro* transcribed mutants of RNase MRP RNA (see Fig. 5) and after precipitation by glutathione–Sepharose, co-precipitated RNAs were analysed by gel electrophoresis and autoradiography. In all panels, lane 1 shows the mixture of radiolabelled input RNAs and lane 2 the negative control precipitation with GST. Lane 3 contains the RNAs precipitated by GST–hPop1 (**A**), GST–Rpp20 (**B** and **C**) and lane 4 contains the RNAs precipitated by GST–Rpp25 (B) or GST-Rpp38 (C), respectively.

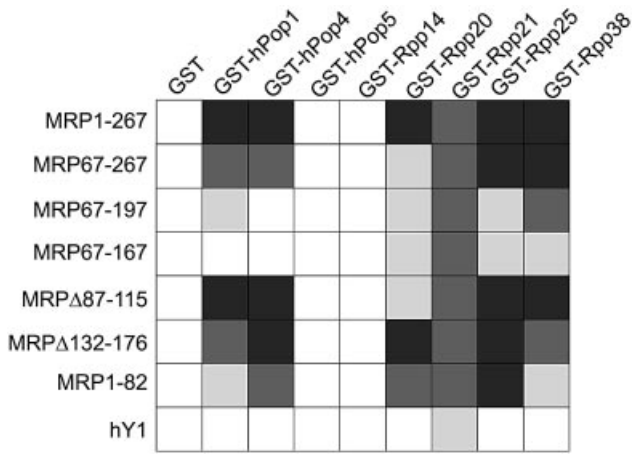

Figure 7. Summary of protein–RNA interactions between the RNase MRP subunits detected by GST pull-down analyses. The efficiency of binding by the GST-fusion proteins to the deletion mutants of RNase MRP RNA was determined by three independent experiments. The most efficient interactions are indicated by dark-grey boxes, intermediate interactions by grey boxes and weak interactions by light-grey boxes. In agreement with the lack of interaction with the full-length RNase MRP RNA (Fig. 4), GST–hPop5 and GST–Rpp14 did not shown detectable interactions with any of the RNase MRP RNA mutants.

found in the two-hybrid system. The failure to detect the hPop4 (Rpp29)–Rpp38 and hPop4–hPop4 interactions in the yeast two-hybrid system may be due to interference by the fused DNA-binding and/or transcription activation domains. Most of the very weak interactions in the yeast two-hybrid system were not observed in the GST pull-down assay. A systematic two-hybrid analysis was also performed for the protein subunits of the yeast RNase P complex (28). Interestingly, two of the strong interactions we observed, hPop1–hPop4 and hPop4–hPop5, were also reported for their yeast counterparts. The failure to detect all the other strong and moderate interactions observed for the human RNase P/RNase MRP subunits in yeast can be explained by the fact that these concern Rpp14, Rpp25, Rpp38 and Rpp40, for which no yeast orthologues are known. It should be stressed that due to the experimental approach, both the yeast two-hybrid system and the GST pull-down assay, the detection of some interactions might have failed because in both cases at least one of the interacting partners is used as a fusion protein and the fusion part may interfere with the interaction. Nevertheless, we conclude that our data provide important and useful new insights into the assembly of protein subunits in the RNase P and RNase MRP complexes.

The most efficient protein–protein interaction observed in our experiments was that between Rpp20 and Rpp25: close to 100% of *in vitro* translated protein added bound to the GST-tagged partner. The stability of the interaction between Rpp20 and Rpp25 was substantiated by increasing the salt concentration in the pull-down assay. KCl concentrations up to 3 M hardly affected the efficiency of this interaction. Recently, it has been reported that both Rpp20 and Rpp25 are members of the Alba superfamily of proteins, an ancient family of nucleic acid-binding proteins that has evolved to support a diversity of functions in RNA metabolism (32).

An interesting phenomenon is the putative homodimerization of hPop1 and hPop4, as suggested by our GST pull-down data. Homodimerization (or multimerization) of RNase MRP/P protein subunits is supported by yeast two-hybrid data on both the human and the yeast RNase MRP/RNase P proteins (26,28). While homodimerization of Pop1 and Pop4 was observed for the human and yeast proteins, respectively,

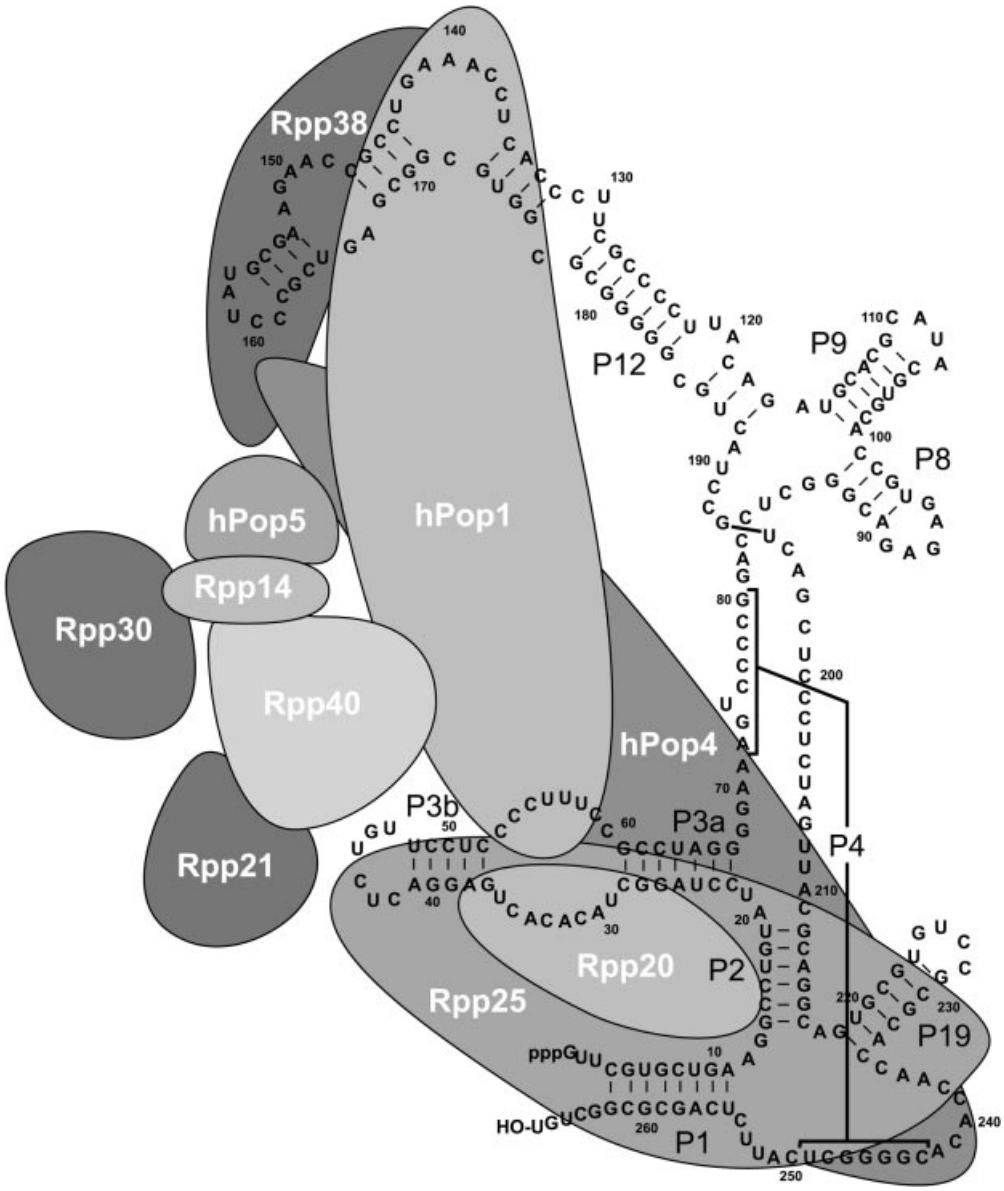

Figure 8. Model for the human RNase MRP complex. Using the data obtained in this study and previously published UV-crosslinking data (25), a structural model for the human RNase MRP complex was generated. In this model, all detected protein–RNA interactions, except for the interaction of Rpp21, which seemed to be non-specific, are combined with all detected protein–protein interactions, except for the most weak interactions. Note that the size of the depicted subunits is not proportional to their molecular masses.

Rpr2–Rpr2 (the yeast counterpart of Rpp21) and Rpp30–Rpp30 and Rpp38–Rpp38 interactions were reported as well. Because little information is available on the protein stoichiometry in the human RNase MRP/P complexes, the physiological relevance of these interactions remains to be investigated. In this respect it is interesting to note that small subpopulations of RNase P and RNase MRP have been proposed to associate with each other (33).

Protein–RNA interactions

Previous UV-crosslinking and yeast three-hybrid analyses have demonstrated that Rpp20, Rpp21, Rpp25, Rpp30 and Rpp38 interact directly with the RNA subunit of human RNase P and/or RNase MRP. Also, Pop1p and Pop4p, the *S.cerevisiae* homologs of hPop1 and hPop4, were shown to interact directly with yeast RNase P RNA in a yeast three-hybrid system (25,27,28). Our GST pull-down analyses indeed confirm that these proteins can directly interact with the RNase MRP RNA, whereas hPop5 and Rpp14 can not. Due to the failure to express GST-fusion proteins for Rpp30 and Rpp40, we were unable to analyse these protein subunits in this assay. Surprisingly, hPop4 only detectably interacted with the RNase MRP RNA in the absence of magnesium ions (data not shown). Mg^{2+} concentrations of 2 mM already precluded the interaction of hPop4 with full-length RNase MRP and RNase P RNA, whereas the RNA binding by the other RNase MRP/P subunits was not affected by magnesium concentrations up to 5 mM. This suggests that direct contacts between

hPop4 and the RNase MRP or RNase P RNA are highly conformation dependent. Because hPop4 also displayed a number of strong protein–protein interactions with other RNase MRP subunits, this raises the question as to whether the binding of these subunits to the RNA may facilitate the formation of bonds between hPop4 and RNase MRP RNA in the presence of magnesium ions. Additional structural analyses will be required to shed more light on this issue. Recently, the NMR structure of an archaeal Rpp29 (Pop4) protein has been solved (34). The *Archaeoglobus fulgidus* Rpp29 protein was found to consist of a six-stranded anti-parallel β-sheet, carrying several conserved hydrophilic amino acids on its surface, which are likely to be involved in intermolecular contacts with other protein and RNA components.

Our mutant RNase MRP RNA analyses demonstrated that hPop1 contacts multiple regions of the RNA, including the P3 and P12 regions and suggest that the P4 region is critically important. The requirement for multiple regions of the human MRP RNA for the association of hPop1 is consistent with the results of reconstitution experiments in HeLa cell extracts (25). Previously, the results of UV-crosslinking experiments indicated that the binding of Rpp20 and Rpp25 to the RNase MRP RNA was critically dependent on the region bordered by nucleotides 22 and 66 (P3 region) (25). The data described here show that in addition to the P3 region, the P8/P9 region is required for the stable association of Rpp20, whereas the RNA seems to contain two independent binding sites for Rpp25, one in the P3 region and a second one in the P4/P19 region. The apparent discrepancy between the results for Rpp25 association with fragment 67–267 (containing the P4/P19 region) of the RNase MRP RNA as obtained by UV-crosslinking in HeLa cell extracts on the one hand and GST pull-down experiments on the other hand, may be due to UV-crosslinking efficiency to the Rpp25 binding site in this region, masking of Rpp25 epitopes when bound to the P4/P19 region, or to conformational changes in the mutant RNA induced by HeLa cell factors. Our hPop4 data show that the binding of hPop4 to the RNase MRP RNA is strongly dependent on the presence of the P3 domain. The deletion of the region between nucleotides 198 and 267 in addition to the P3 domain completely abolished hPop4 binding. These data are consistent with the involvement of the P4/P19 region, in addition to the P3 region, in the interaction between hPop4 and RNase MRP RNA. In agreement with previous UV-crosslinking and reconstitution-co-immunoprecipitation data, our GST pull-down data indicate that the main determinants for the binding of Rpp38 are located in the P12 region. In spite of the limited degree of primary and secondary structure homology between this region of the RNA components of RNase MRP and RNase P, Rpp38 stably interacts with both of them. Therefore, it will be interesting to investigate the high-resolution structures of these RNA domains, as well as the nucleotides and amino acids which are directly involved in the interaction of Rpp38 with these RNA molecules. The RNase MRP RNA has been suggested to contain a kink–turn motif, a protein binding module found in a variety of other RNAs (35). Interestingly, a major part of the Rpp38 protein shows 32% homology with the kink–turn binding ribosomal L7Ae protein of *Haloarcula marismortui*. Although these data suggest that Rpp38 binds to a kink–turn structure in RNase MRP RNA, such a motif cannot be discerned in the RNase P RNA. Detailed structural analyses of both protein and RNA subunits will be required to investigate this intriguing issue.

Human RNase MRP model

The mutual interactions among RNase MRP/P subunits allowed us to generate a structural model for the human RNase MRP complex. The model displayed in Figure 8 is based upon all protein–RNA and the most efficient protein–protein interactions detected in the present study. This model provides new insights into the assembly of the complex. In addition, it will be useful in studying the role of single subunits in RNase MRP function and will provide a basis for RNase MRP reconstitution experiments. Recently, the first *in vitro* reconstitution experiments for the human RNase P complex were reported by Mann and colleagues (36). The results demonstrated that the reconstitution of a particle composed of the RNase P RNA and recombinant Rpp21 and hPop4 generated a functionally active complex. Future studies will be needed to investigate to what extent our results for RNase MRP can be extrapolated to RNase P and whether a similarly reconstituted RNase MRP particle will be active as well.

SUPPLEMENTARY MATERIAL

Supplementary Material is available at NAR Online.

ACKNOWLEDGEMENTS

The authors thank David Tollervey (University of Edinburgh, Scotland, UK), Sidney Altman, Cecilia Guerrier-Takada (Yale University, New Haven, CT, USA) and Nayef Jarrous (Hebrew University-Hadassah Medical School, Jerusalem, Israel) for their kind gifts of cDNAs encoding hRrp42p and RNase P protein subunits. Furthermore, we want to thank Reinout Raijmakers for critical reading of the manuscript. This work was supported in part by the Council for Chemical Sciences of the Netherlands Organization for Scientific Research (NWO-CW).

REFERENCES

1. Chang,D.D. and Clayton,D.A. (1987) A novel endoribonuclease cleaves at a priming site of mouse mitochondrial DNA replication. *EMBO J.*, **6**, 409–417.
2. Kiss,T., Marshallsay,C. and Filipowicz,W. (1992) 7-2/MRP RNAs in plant and mammalian cells: association with higher order structures in the nucleolus. *EMBO J.*, **11**, 3737–3746.
3. Topper,J.N. and Clayton,D.A. (1990) Characterization of human MRP/Th RNA and its nuclear gene: full length MRP/Th RNA is an active endoribonuclease when assembled as an RNP. *Nucleic Acids Res.*, **18**, 793–799.
4. Lygerou,Z., Allmang,C., Tollervey,D. and Seraphin,B. (1996) Accurate processing of a eukaryotic precursor ribosomal RNA by ribonuclease MRP *in vitro*. *Science*, **272**, 268–270.
5. Chang,D.D. and Clayton,D.A. (1987) A mammalian mitochondrial RNA processing activity contains nucleus-encoded RNA. *Science*, **235**, 1178–1184.
6. Terns,M.P. and Terns,R.M. (2002) Small nucleolar RNAs: versatile trans-acting molecules of ancient evolutionary origin. *Gene Expr.*, **10**, 17–39.
7. Tollervey,D. and Kiss,T. (1997) Function and synthesis of small nucleolar RNAs. *Curr. Opin. Cell Biol.*, **9**, 337–342.

8. Kiss-Laszlo,Z., Henry,Y., Bachellerie,J.P., Caizergues-Ferrer,M. and Kiss,T. (1996) Site-specific ribose methylation of preribosomal RNA: a novel function for small nucleolar RNAs. *Cell*, **85**, 1077–1088.
9. Ganot,P., Bortolin,M.L. and Kiss,T. (1997) Site-specific pseudouridine formation in preribosomal RNA is guided by small nucleolar RNAs. *Cell*, **89**, 799–809.
10. van Eenennaam,H., Jarrous,N., van Venrooij,W.J. and Pruijn,G.J. (2000) Architecture and function of the human endonucleases RNase P and RNase MRP. *IUBMB Life*, **49**, 265–272.
11. Jarrous,N. (2002) Human ribonuclease P: subunits, function and intranuclear localization. *RNA*, **8**, 1–7.
12. Reddy,R. and Shimba,S. (1995) Structural and functional similarities between MRP and RNase P. *Mol. Biol. Rep.*, **22**, 81–85.
13. Forster,A.C. and Altman,S. (1990) Similar cage-shaped structures for the RNA components of all ribonuclease P and ribonuclease MRP enzymes. *Cell*, **62**, 407–409.
14. Collins,L.J., Moulton,V. and Penny,D. (2000) Use of RNA secondary structure for studying the evolution of RNase P and RNase MRP. *J. Mol. Evol.*, **51**, 194–204.
15. Ridanpaa,M., van Eenennaam,H., Pelin,K., Chadwick,R., Johnson,C., Yuan,B., vanVenrooij,W., Pruijn,G., Salmela,R., Rockas,S. *et al.* (2001) Mutations in the RNA component of RNase MRP cause a pleiotropic human disease, cartilage-hair hypoplasia. *Cell*, **104**, 195–203.
16. Ridanpaa,M., Sistonen,P., Rockas,S., Rimoin,D.L., Makitie,O. and Kaitila,I. (2002) Worldwide mutation spectrum in cartilage-hair hypoplasia: ancient founder origin of the major70A→G mutation of the untranslated RMRP. *Eur. J. Hum. Genet.*, **10**, 439–447.
17. Lygerou,Z., Pluk,H., van Venrooij,W.J. and Seraphin,B. (1996) hPop1: an autoantigenic protein subunit shared by the human RNase P and RNase MRP ribonucleoproteins. *EMBO J.*, **15**, 5936–5948.
18. van Eenennaam,H., Pruijn,G.J. and van Venrooij,W.J. (1999) hPop4: a new protein subunit of the human RNase MRP and RNase P ribonucleoprotein complexes. *Nucleic Acids Res.*, **27**, 2465–2472.
19. van Eenennaam,H., Lugtenberg,D., Vogelzangs,J.H., van Venrooij,W.J. and Pruijn,G.J. (2001) hPop5, a protein subunit of the human RNase MRP and RNase P endoribonucleases. *J. Biol. Chem.*, **276**, 31635–31641.
20. Jarrous,N., Eder,P.S., Wesolowski,D. and Altman,S. (1999) Rpp14 and Rpp29, two protein subunits of human ribonuclease P. *RNA*, **5**, 153–157.
21. Jarrous,N., Eder,P.S., Guerrier-Takada,C., Hoog,C. and Altman,S. (1998) Autoantigenic properties of some protein subunits of catalytically active complexes of human ribonuclease P. *RNA*, **4**, 407–417.
22. Jarrous,N., Reiner,R., Wesolowski,D., Mann,H., Guerrier-Takada,C. and Altman,S. (2001) Function and subnuclear distribution of Rpp21, a protein subunit of the human ribonucleoprotein ribonuclease P. *RNA*, **7**, 1153–1164.
23. Guerrier-Takada,C., Eder,P.S., Gopalan,V. and Altman,S. (2002) Purification and characterization of Rpp25, an RNA-binding protein subunit of human ribonuclease P. *RNA*, **8**, 290–295.
24. Eder,P.S., Kekuda,R., Stolc,V. and Altman,S. (1997) Characterization of two scleroderma autoimmune antigens that copurify with human ribonuclease P. *Proc. Natl Acad. Sci. USA*, **94**, 1101–1106.
25. Pluk,H., van Eenennaam,H., Rutjes,S.A., Pruijn,G.J. and van Venrooij,W.J. (1999) RNA–protein interactions in the human RNase MRP ribonucleoprotein complex. *RNA*, **5**, 512–524.
26. Jiang,T. and Altman,S. (2001) Protein–protein interactions with subunits of human nuclear RNase P. *Proc. Natl Acad. Sci. USA*, **98**, 920–925.
27. Jiang,T., Guerrier-Takada,C. and Altman,S. (2001) Protein–RNA interactions in the subunits of human nuclear RNase P. *RNA*, **7**, 937–941.
28. Houser-Scott,F., Xiao,S., Millikin,C.E., Zengel,J.M., Lindahl,L. and Engelke,D.R. (2002) Interactions among the protein and RNA subunits of *Saccharomyces cerevisiae* nuclear RNase P. *Proc. Natl Acad. Sci. USA*, **99**, 2684–2689.
29. Frangioni,J.V. and Neel,B.G. (1993) Solubilization and purification of enzymatically active glutathione S-transferase (pGEX) fusion proteins. *Anal. Biochem.*, **210**, 179–187.
30. Pruijn,G.J., Slobbe,R.L. and van Venrooij,W.J. (1991) Analysis of protein–RNA interactions within Ro ribonucleoprotein complexes. *Nucleic Acids Res.*, **19**, 5173–5180.
31. Raijmakers,R., Noordman,Y.E., van Venrooij,W.J. and Pruijn,G.J. (2002) Protein–protein interactions of hCsl4p with other human exosome subunits. *J. Mol. Biol.*, **315**, 809–818.
32. Aravind,L., Iyer,L.M. and Anantharaman,V. (2003) The two faces of Alba: the evolutionary connection between proteins participating in chromatin structure and RNA metabolism. *Genome Biol.*, **4**, R64.
33. Lee,B., Matera,A.G., Ward,D.C. and Craft,J. (1996) Association of RNase mitochondrial RNA processing enzyme with ribonuclease P in higher ordered structures in the nucleolus: a possible coordinate role in ribosome biogenesis. *Proc. Natl Acad. Sci. USA*, **93**, 11471–11476.
34. Sidote,D.J. and Hoffman,D.W. (2003) NMR structure of an archaeal homologue of ribonuclease p protein rpp29. *Biochemistry*, **42**, 13541–13550.
35. Klein,D.J., Schmeing,T.M., Moore,P.B. and Steitz,T.A. (2001) The kink–turn: a new RNA secondary structure motif. *EMBO J.*, **20**, 4214–4221.
36. Mann,H., Ben Asouli,Y., Schein,A., Moussa,S. and Jarrous,N. (2003) Eukaryotic RNase P: role of RNA and protein subunits of a primordial catalytic ribonucleoprotein in RNA-based catalysis. *Mol. Cell*, **12**, 925–935.
37. Frank,D.N., Adamidi,C., Ehringer,M.A., Pitulle,C. and Pace,N.R. (2000) Phylogenetic-comparative analysis of the eukaryal ribonuclease P RNA. *RNA*, **6**, 1895–1904.